Design and synthesis of 4,5,6,7-tetrahydro-1*H*-1,2-diazepin-7-one derivatives as a new series of Phosphodiesterase 4 (PDE4) inhibitors

Sara Guariento, Anna Karawajczyk, James A. Bull, Gessica Marchini, Martyna Bielska, Xenia Iwanowa, Olga Bruno, Paola Fossa, Fabrizio Giordanetto

PII: S0960-894X(16)31193-3
DOI: http://dx.doi.org/10.1016/j.bmcl.2016.11.040
Reference: BMCL 24435

To appear in: *Bioorganic & Medicinal Chemistry Letters*

Received Date: 3 October 2016
Revised Date: 14 November 2016
Accepted Date: 15 November 2016

Please cite this article as: Guariento, S., Karawajczyk, A., Bull, J.A., Marchini, G., Bielska, M., Iwanowa, X., Bruno, O., Fossa, P., Giordanetto, F., Design and synthesis of 4,5,6,7-tetrahydro-1*H*-1,2-diazepin-7-one derivatives as a new series of Phosphodiesterase 4 (PDE4) inhibitors, *Bioorganic & Medicinal Chemistry Letters* (2016), doi: http://dx.doi.org/10.1016/j.bmcl.2016.11.040

Design and synthesis of 4,5,6,7-tetrahydro-1*H*-1,2-diazepin-7-one derivatives as a new series of Phosphodiesterase 4 (PDE4) inhibitors.

Sara Guariento[a], Anna Karawajczyk[b], James A. Bull[b], Gessica Marchini[c], Martyna Bielska[b], Xenia Iwanowa[b], Olga Bruno[a], Paola Fossa[a], Fabrizio Giordanetto[b,§,*]

[a]Department of Pharmacy, University of Genoa, Viale Benedetto XV n. 3, 16132, Genoa, Italy

[b]Medicinal Chemistry, Taros Chemicals GmbH & Co. KG, Emil-Figge-Str. 76a, 44227 Dortmund, Germany

[c]Pharmacology Toxicology Department, Chiesi Farmaceutici S.p.A., Nuovo Centro Ricerche, Largo Belloli 11/a, 43122 Parma, Italy

[§]Present address: DE Shaw Research, 120W 45th Street, New York, 10036, United States of America

*Corresponding Author:

Tel: +1 (0)212 4780 822; e-mail: fabrizio.giordanetto@deshawresearch.com

Keywords

Phosphodiesterase 4, PDE4 inhibitors, diazepinone derivatives, compound library

Abstract

Phosphodiesterase 4 (PDE4) inhibitors have attractive therapeutic potential in respiratory, inflammatory, metabolic and CNS disorders. The present work details the design, chemical exploration and biological profile of a novel PDE4 inhibitor chemotype. A diazepinone ring was identified as an under-represented heterocyclic system fulfilling a set of PDE4 structure-based design hypotheses. Rapid exploration of the structure activity relationships for the series was enabled by robust and scalable two/three-steps parallel chemistry protocols. The resulting compounds demonstrated PDE4 inhibitory activity in cell free and cell-based assays comparable to the Zardaverine control used, suggesting potential avenues for their further development.

Phosphodiesterase 4 (PDE4) belong to the superfamily of 3',5'-cyclic-nucleotide Phosphodiesterase and catalyse the hydrolysis of cyclic adenosine 3',5'monophosphate (cAMP) to its inactive 5'-monophosphate metabolite, thus blocking the associated signal transduction systems.[1]

The PDE4 family consists of 4 isoforms (named A, B, C and D) and 25 splice variants,[2,3] which display a highly conserved catalytic site (78% of similarity).[4] Distinct promoters and mechanisms control the mRNA stability of the various PDE4 variants therefore allowing a fine-tuned regulation and compartmentalisation of the formed isoforms and c-AMP intracellular levels.[5-7]

In particular, PDE4s are mainly found in inflammatory cells, brain, pulmonary and vascular smooth muscle cells and cardiovascular tissue both at cytosolic and plasmatic membrane level.[8-9] In those tissues, the intracellular concentration of cAMP modulates inflammatory processes such as cellular trafficking and adhesion, cytokine and chemokine release, the production of reactive oxygen species, the secretion of mucus in the respiratory tract and the airway smooth muscle contraction.[8,10] In the central nervous system (CNS), cAMP is involved in regulating synaptic plasticity and memory formation, by promoting the activation of cAMP response element-binding protein (CREB)[11] and the expression of neurotrophic factor, which enhance progenitor cell proliferation in hippocampus and axonal growth.[12-14] An excessive degradation of cAMP promotes inflammatory diseases and CNS disorders, where behavioural, learning and memory processes are affected.[7]

Therefore, increasing intracellular cAMP via PDE4 inhibition has been pursued for decades as an appealing strategy for the treatment of inflammation-related respiratory diseases such as Chronic Obstructive Pulmonary Disease (COPD), asthma, allergic rhinitis

and idiopathic pulmonary fibrosis.[16,17,18] More recently, PDE4 inhibition also demonstrated positive effects against aberrant immune response diseases, such as atopic dermatitis, rheumatoid arthritis, multiple sclerosis, psoriasis and lupus erythematosus.[9,19,20] Further studies using archetypical PDE4 inhibitors (e.g. Resveratrol,[21] Rolipram [22] and Roflumilast[23]) have also implicated these enzymes in the modulation of metabolic disorders such as obesity, type 2 diabetes and metabolic syndrome, and glomerulonephritis, as they all share an underlying inflammatory component.[9,24,25] The therapeutic potential of PDE4 inhibition in pulmonary artery hypertension, renal transplantation and renal failure was also reported.[9] Finally, the influence of PDE4s on long term potentiation of the synaptic activity and on neuronal plasticity in general,[26,27] as well as the beneficial effect of PDE4 inhibitors on depression, tissue injury and neurodegeneration[12,13] are well documented.

Among the wide variety of compounds active against this enzyme,[28] Rolipram, Cilomilast,[29] Roflumilast and Apremilast[30] (Figure 1) are some of the most characterised PDE4 inhibitors to date. It is noteworthy that Roflumilast and Apremilast were approved by the Food and Drug Administration (FDA) as oral drugs for the treatment of COPD and psoriatic arthritis in 2011[23] and 2014,[31] respectively.

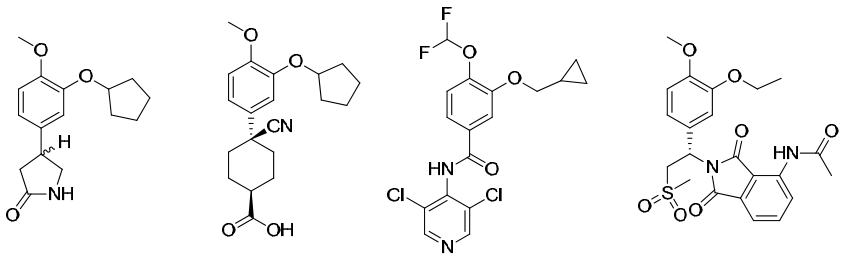

Rolipram, IC_{50}: 1 μM

Cilomilast, IC_{50}: 70 nM

Roflumilast, IC_{50}: 0.6 nM

Apremilast, IC_{50}: 74 nM

Figure 1. Molecular structure of selected PDE4 inhibitors: Rolipram, Cilomilast, Roflumilast, Apremilast.

Despite these successes, the development of novel PDE4 inhibitors is typically hampered by the occurrence of dose-limiting side effects like nausea, emesis, sedation[18,32,33] and novel chemical starting points are required to seed future drug discovery efforts.

Data mining of the scientific and patent literature indicated a large body of chemical matter developed towards PDE4A-D inhibition, for a total of 5537 unique compounds with measured PDE4 inhibition. Chemoinfomatics analysis of this data set served to identify and compare various chemotypes with the aim to identify suitable starting points for additional chemical exploration. Here, a cluster of catechol-containing cyclic hydrazides was found to be of particular relevance due to the relatively high PDE4 inhibition, adequate efficiency parameters (i.e. ligand efficiency (LE) and ligand lipophilicity efficiency (LLE)) and available structural biology data, as shown by selected examples in Figure 2. This molecular cluster included the archetypical PDE4 inhibitor Zardaverine (IC_{50}: 1.41 μM) [34], whose binding mode to the enzyme has been elucidated (PDB code: 1XOR)[35]. As shown in Figure 3A, Zardaverine establishes productive polar interactions with the catalytic site: a) bi-dentate hydrogen bond between the catechol's oxygen atoms and the side chain of Q369, a pivotal residue in the interaction with c-AMP and with PDE4 inhibitors in general,[35] b) coordination of the Zinc ion and hydrogen bond to H160 via the pyridazinone ring's oxygen (displacing one of the six conserved coordinated waters of the PDE4 active site)[35] and nitrogen atoms, respectively.

Interestingly, the pyridazinone moiety of Zardaverine is surrounded by two side pockets, the so called S pocket[35] (including G206, S208, E339, F340, Q343, S355, C358)

and a smaller one (including L319, S320, N321), as highlighted in Figure 3. We reasoned both of them could be exploited to engage additional interactions with the enzyme and optimize the functional potency of the inhibitors. Indeed, analogous cyclic hydrazides such as tetrahydrophtalazinone **2**[36] and 4,4-dimethylpyrazolone **3**,[37] showed favourable PDE4 inhibition results (Figure 2) suggesting opportunities for further chemical diversification in the area. We thus designed a 4,5,6,7-tetrahydro-1*H*-1,2-diazepin-7-one ring as a likely scaffold satisfying this structure-based framework as summarized in Figure 2.

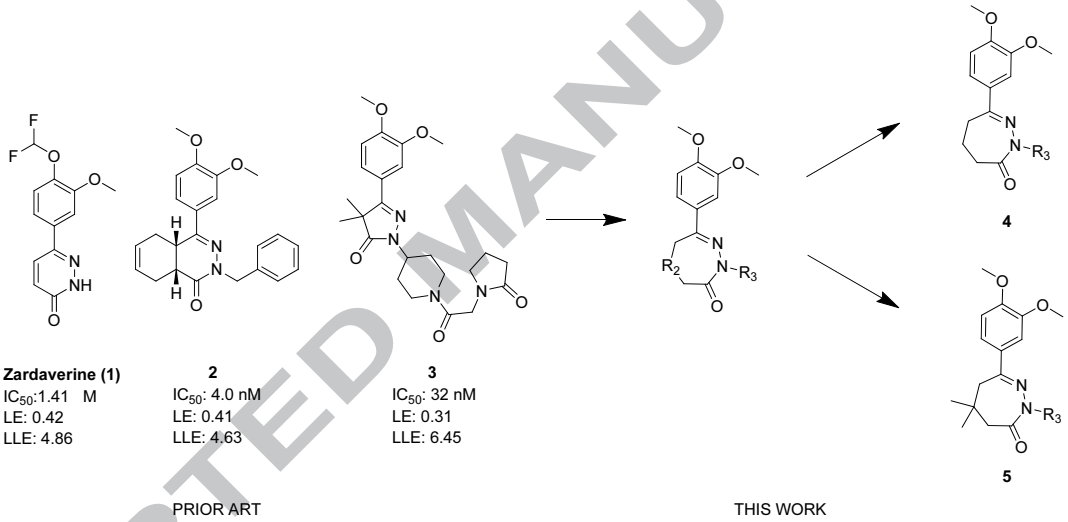

Figure 2. Design process underpinning the present work. IC_{50} values for Zardaverine (this work), **2**[34] and **3**[35] are indicated. Ligand efficiency (LE) was calculated as 1,37*-log10(PDE4 IC_{50})/Heavy Atom Count (HAC) and Ligand lipophilicity efficiency (LLE) was calculated as -log10(PDE4 IC_{50})- clogP. clogP was calculated with ChemDraw®.

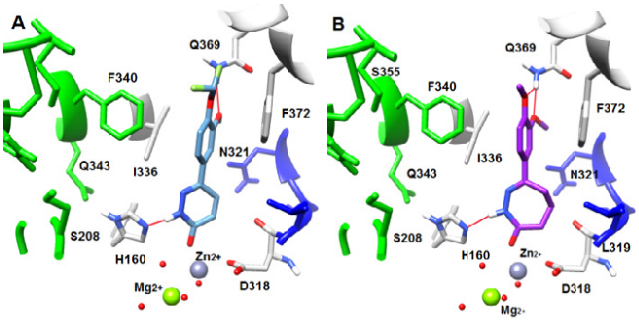

Figure 3. (A) Experimental binding modes of Zardaverine (PDB code:1XOR). (B) Predicted binding mode of **4**. Amino acid residues from the S pocket are colored in green, while residues from the smaller side pocket are colored in blue. The Zinc and Magnesium ions are represented as grey and green spheres, respectively. Water molecules are shown as red spheres. H-bonds between the compounds and the active site amino acids are highlighted as red solid lines.

Importantly, the seven-membered ring nature of the intended scaffold served multiple purposes: a) it would allow for a pragmatic, lipophilicity efficient steric extension toward the smaller side pocket b) it could be rapidly assembled and diversified using robust synthetic chemistry protocols and c) it offered an opportunity to explore an innovative, underrepresented heterocyclic chemical space as only 25 tetrahydro-[1,2]-diazepinone derivatives have been described to date,[38] none of which in the context of PDE4 inhibition. Based on these premises, the dimethoxyphenyl moiety substituting C3 of the 4,5,6,7-tetrahydro-1*H*-1,2-diazepin-7-one ring was maintained due to its PDE4 warhead character. Two additional diversification elements at the C5 and N1 position of the designed scaffold were considered (Figure 2). Here, C5 included a methylene and a *geminal*-dimethyl group to further extend towards the end of the smaller side pocket. On

N1, a wider range of alkyl substituents could be introduced following robust N-alkylation protocols in a parallel chemistry format to verify structure activity relationships (SAR) at the S pocket. Selection of appropriate side chains was informed by a combination of chemical diversity and physicochemical properties considerations.[39,40] In particular, docking calculations were performed to assess binding of the 3-(3,4-dimethoxyphenyl)-4,5,6,7-tetrahydro-1*H*-1,2-diazepin-7-one **4** and 3-(3,4-dimethoxyphenyl)-5,5-dimethyl-4,5,6,7-tetrahydro-1*H*-1,2-diazepin-7-one **5** within PDE4 active site (Figure 3). The aforementioned crystal structure of PDE4 active site in complex with Zardaverine (PDB code: 1XOR) was selected for the simulations. **4** and **5** displayed a comparable binding mode to Zardaverine (with compound **4** showing the best docking score, Table 1) maintaining key hydrogen bonds to the side chains of H160 and Q369. (Figure 3B).

We therefore synthesized 3-(3,4-dimethoxyphenyl)-5,6-dihydro-1*H*-1,2-diazepin-7(4*H*)-one **4** and 3-(3,4-dimethoxyphenyl)-5,5-dimethyl-5,6-dihydro-1*H*-1,2-diazepin-7(4*H*)-one **5** to establish comparison baselines to Zardaverine and verify any PDE4 inhibition difference across scaffolds. Compounds **6**, where the catechol moiety of Zardaverine was replaced by 4-methoxyphenyl served as a negative control for the structure-based hypothesis (Figure 3). A one-step Friedel-Crafts acylation between phenyl derivatives **7, 8** and anhydrides **9, 10** yielded the acid intermediates **11-13** in 41% to 92% yields (Scheme 1). Interestingly, the reactivity of the two anhydrides was different. Using **10** the reaction proceeded to completion in 1h and longer reaction time using **8** as starting material led to the de-methylation of one of the two phenolic oxygens. The same side reaction occurred with **9** only after 12 h. Presence of diphenyl-containing side product was detected, which was easily removed by an acid-base extraction (ethyl acetate/10%

sodium hydroxide aqueous solution followed by ethyl acetate/1N hydrochloric acid aqueous solution).

The cyclization reaction of the formed 5-oxopentanoic acids **11-13** was executed with hydrazine hydrate at 150 °C (Scheme 2). By using a Dean-Stark apparatus, water content in the reaction mixture was minimized, firstly promoting the formation of the hydrazone and then avoiding the hydrolysis of the final hydrazide.[41] This cyclization was overall low-yielding (13 □ 85%) and represented the limiting step of the synthetic route. Its success rate was greatly influenced by the choice of the R_2 substituents (Scheme 2): the insertion of the *geminal*-CH_3 in 5 (**5**) underwent the cyclisation with the best yield, following a typical Thorpe-Ingold effect.[42]

Scheme 1. Synthesis of intermediates **11**-**13**.

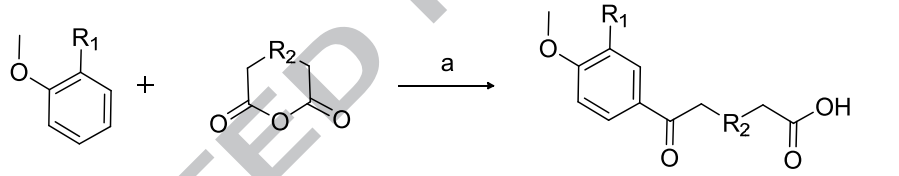

7:R_1 = H
8:R_1 = OCH_3
9:R_2 = CH_2
10:R_2 = *gem*-CH_3

11: R_1 = OCH_3, R_2= CH_2 (92%)
12: R_1 = OCH_3, R_2 = *gem*-CH_3 (41%)
13: R_1 = H, R_2 = CH_2 (46%)

Reagents and conditions: (a) $AlCl_3$, dry DCM, rt, 1 □ 10 h.

Scheme 2. Synthesis of final compounds **4**-**6**.

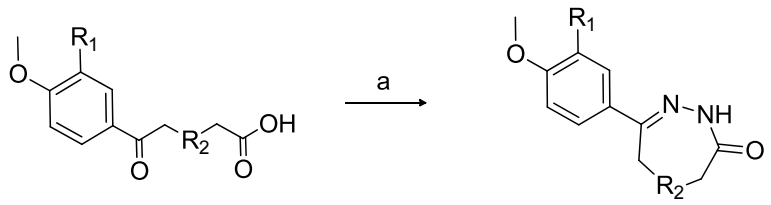

11: R_1 =OCH_3, R_2= CH_2
12: R_1 =OCH_3, R_2 =*gem*-CH_3
13: R_1 =H, R_2 =CH_2

4: R_1 =OCH_3, R_2= CH_2 (13%)
5: R_1 =OCH_3, R_2 = *gem*-CH_3 (85%)
6: R_1 =H, R_2 =CH_2 (18%)

Reagents and conditions: (a) NH_2NH_2 hydrate, xylene, reflux, 5 h.

As shown in Table 1, **4** and **5** showed comparable PDE4B2 inhibition to Zardaverine, lending support to the chosen design approach (Table 1). The dramatic loss of potency of **6** (PDE4B2 IC_{50} > 30 μM) highlighted the importance of the bi-dentate H bond between the two catechol oxygen atoms and Q369 as a necessary interaction with the enzyme. Interestingly, the addition of the *geminal*-CH_3 in 5 of the diazepinone did not result in a potency gain consistent with the increased size and lipophilicity (cf. **5** and **4**). Having confirmed the 4,5,6,7-tetrahydro-1*H*-1,2-diazepin-7-one scaffold as an effective PDE4 inhibitor starting point, we proceeded to the functionalization of its N1 position to verify how different substituents could affect PDE4 inhibition. Three 5,5-dimethyl-4,5,6,7-tetrahydro-1*H*-1,2-diazepin-7-one substituted examples were also synthesized as a further validation for the 5-*geminal*-dimethyl substitution.

Table 1. PDE4B2 inhibition potency and ligand efficiency parameters for compounds **4-6**.

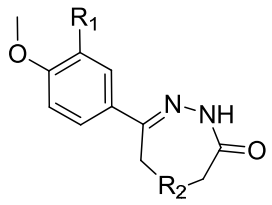

Entry	R_1	R_2	PDE4B2 IC_{50} (μM)[a]	LE[b]	LLE[c]	Docking Score[d]
Zardaverine	-	-	1.41	0.42	4.86	-24.5415
4	OCH_3	CH_2	4.17	0.41	4.32	-29.6783
5	OCH_3	*gem*-CH_3	3.53	0.37	3.36	-24.9914
6	H	CH_2	>30	-	-	-

[a] Results are mean of at least two experiments, assay variability within 25% of reported value.. [b] Ligand efficiency (LE) was calculated as 1,37*-$\log_{10}$(PDE4B2 IC_{50})/Heavy Atom Count (HAC). [c] Ligand lipophilicity efficiency (LLE) was calculated as -$\log_{10}$(PDE4B2 IC_{50})- clogP. clogP was calculated with ChemDraw®. [d]Docking scores were calculated with FlexX as implemented in LeadIT® (Supporting Material).

The alkylation of the diazepinone ring (Scheme 3) was performed in a parallel format with a 24 position Mettler-Toledo Miniblock® apparatus, by using the relevant alkyl bromide or iodide and a 60% dispersion of sodium hydride in mineral oil at room temperature.[43]This set-up allowed the production of fifteen final compounds in adequate quantity (at least 2 mg) and purity (liquid chromatography-mass spectrometry (LC-MS >85%)) for further biochemical profiling (Table 2 and 3).

Scheme 3. Synthesis of final compounds **14-28.**

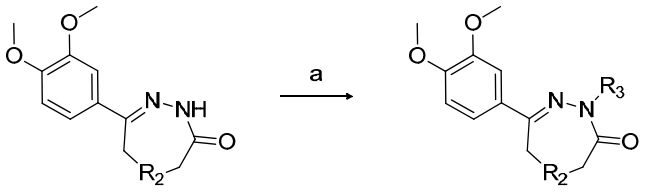

11: R_2= CH_2
12: R_2 = *gem*-CH_3

14-28 (>60%)

Reagents and conditions: (a) R_3X, NaH 60% in mineral oil, DMF, rt, 2 h.

Table 2. PDE4B2 inhibition potency and efficiency for compounds **14-25**.

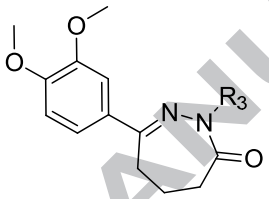

Entry	R_3	PDE4B2 IC_{50} (μM)[a]	LE[b]	LLE[c]
Zardaverine	-	1.41	0.42	4.86
4	H	4.17	0.41	4.32
14	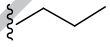	0.26	0.43	4.37
15	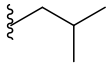	0.34	0.40	3.86
16	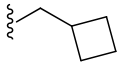	0.32	0.39	3.80
17	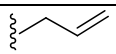	1.13	0.39	4.05
18	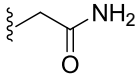	7.55	0.32	4.75
19	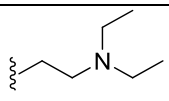	1.62	0.32	3.05
20	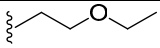	2.27	0.34	3.76

21	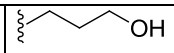	1.22	0.37	5.01
22	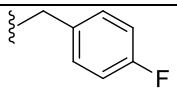	0.17	0.36	3.23
23	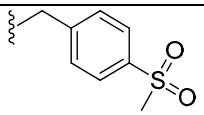	1.29	0.28	4.15
24	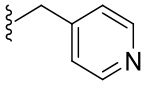	1.41	0.32	3.95
25	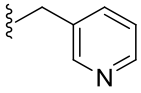	0.29	0.36	4.64

[a] Results are mean of at least two experiments, assay variability within 25% of reported value. [b] Ligand efficiency (LE) was calculated as 1,37*-$\log_{10}$(PDE4B2 IC_{50})/Heavy Atom Count (HAC). [c] Ligand lipophilicity efficiency (LLE) was calculated as -$\log_{10}$(PDE4B2 IC_{50})- clogP. clogP was calculated with ChemDraw®.

Table 3. PDE4B2 inhibition potency and efficiency for compounds **26-28**

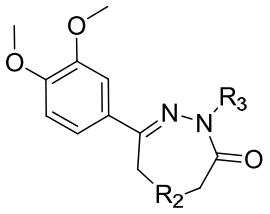

Entry	R_1	R_2	PDE4B2 IC_{50} (μM)[a]	LE[b]	LLE[c]
Zardaverine	-	-	1.41	0.42	4.86
13	*gem*-CH_3	H	3.53	0.37	3.36
19	CH_2	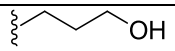	1.22	0.37	5.01
22	CH_2	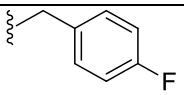	0.17	0.36	3.23

26	*gem*-CH_3	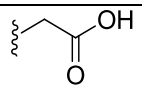	13.08	0.28	2.64
27	*gem*-CH_3	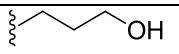	2.69	0.32	3.63
28	*gem*-CH_3	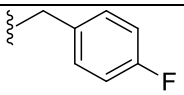	1.22	0.29	1.35

[a]Results are mean of at least two experiments, assay variability within 25% of reported value. [b]Ligand efficiency (LE) was calculated as 1,37*-$\log_{10}$(PDE4B2 IC_{50})/Heavy Atom Count (HAC). [c] Ligand lipophilicity efficiency (LLE) was calculated as -$\log_{10}$(PDE4B2 IC_{50})- clogP. clogP was calculated with ChemDraw®.

Small apolar groups (compounds **14- 17**) appeared to be tolerated overall, with *n*-propyl affording the best inhibitory profile (IC_{50}: 0.26 μM) when normalized by size and lipophilicity (cf. LE and LLE, Table 2). Interestingly, branched and cyclized analogues (**15**, **16**) did not increase potency over the linear counterparts. The introduction of polarity on the N1 side chain, as from amine (**18**) and ether (**19**) linkages or amide (**20**) and alcohol (**21**) functionalities did not have the sought effect on potency, probably due to the lack of rewarding interactions with the PDE4 enzyme.

Incorporation of aryl moieties at N1 via a methylene bridge was more successful from a PDE4 inhibition perspective. Here, **22** and **25** afforded two of the most potent PDE4 inhibitors of this study (IC_{50}: 0.17 and 0.29 μM, respectively). Still, none of the aromatic appendages evaluated were as efficient as the smaller and less lipophilic alkylic substituents (cf. **14** and **15**, Table 2). Interestingly, the 3-pyridylmethyl substituent increased potency ten-fold compared to its "*para*" regioisomer (cf. **24** and **25**), thus hinting at potential directionality effects of substitution for heterocyclic derivatives.

Finally matched pair analysis indicated a general deterioration of PDE4 inhibition for the 5,5-dimethyl-4,5,6,7-tetrahydro-1*H*-1,2-diazepin-7-one scaffold (Table 3), confirming that the insertion of steric bulk at 5 position did not provide any advantage.

The newly designed compounds were able to inhibit the enzymatic activity of PDE4. In particular, **14** offered a 10-fold potency gain and comparable ligand efficiency over Zardaverine. We therefore evaluated the ability of the best compounds so far identified to inhibit the Lipopolysaccharide (LPS)-induced tumor necrosis factor alpha (TNF-α) release in human peripheral blood mononuclear cells (PBMC), a relevant PDE4-based biomarker of functional utility in a clinical setting.[44] Gratifyingly, both **14** and **15** showed significant TNF-α release inhibition (IC_{50}: 0.21 and 0.11 μM, respectively, Table 4), with virtually no drop-off effects from their cell-free IC_{50} values, indicating opportunities for further optimization.

Table 4. Inhibition of LPS-induced TNF-αrelease in human PBMCs for Zardaverine and compounds **14** and **15**

Comp.	PBMC IC_{50} (μM)[a]	LE[b]	LLE[c]
Zardaverine	0.515 (0.098-2.700)	0.45	5.30
14	0.214 (0.072-0.635)	0.44	4.46
15	0.106 (0.052-0.215)	0.43	4.36

[a.] Results are mean of n=1 independent experiment performed in quadruplicate. 95% confidence intervals of the mean are displayed within brackets. [b.] Ligand efficiency (LE) was calculated as 1,37*-$\log_{10}$(PBMC IC_{50})/Heavy Atom Count (HAC). [c] Ligand lipophilicity efficiency (LLE) was calculated as -$\log_{10}$(PBMC IC_{50})- clogP. clogP was calculated with ChemDraw®.

In summary, starting from chemoinformatics analysis of the PDE4 inhibitor prior art, a novel heterocyclic scaffold was designed based on structure-based considerations, diversification opportunities and developability potential. By focussing on the exploration of underrepresented chemical space, a parallel synthetic chemistry protocol was developed using robust and scalable transformations. This resulted in the identification of a series of novel, potent PDE4 inhibitors with promising cellular activity. This preliminary proof of concept coupled with the compact nature of the chemotype formed the basis for its future development and profile optimization.

Author Contributions

The manuscript was written through contributions of all authors.

Notes

The authors declare no competing financial interest.

Acknowledgements

We thank E. Armani for her support in the biological profiling of the compounds.

References

1. Conti, M.; Richter, W.; Mehats, C.; Livera, G.; Park, J.; Jin, C. *J. Biol. Chem.* **2003**, 278, 5493.

2. Houslay, M.D.; Baillie, G.S.; Maurice, D.H. *Circ Res.* **2007**, 100, 950.

3. Houslay, M.D.; Adams, R.D. *Biochem J.* **2003**, 370, 1.

4. Berman, H.M.; Westbrook, J.; Feng, Z.; Gilliland, G.; Bhat, T.N.; Weissig, H.; Shindyalov, I.N.; Bourne, P.E. *Nucleic Acids Res*. **2000**, 28, 235.

5. Keravis, T.; Lugnier, C. *Br. J. Pharmacol*. **2012**, 165, 1288.

6. Fox, D.; Burgin, A.B.; Gurney, M.E. *Cell Signal*, **2014**, 26, 657.

7. Houslay, M.D.; Schafer, P.; Zhang, K.Y.J. *Drug Discovery Today*. **2005**, 10, 1503.

8. Page, G.P.; Spina, D. *Handb Exp Pharmacol*. **2011**, 204, 391.

9. Press, N.J.; Banner, K.H. *Prog Med Chem*. **2009**;47, 37.

10. Castro, A.; Jerez, M.J.; Gil, C.; Martinez, A. *Med. Res. Rev*. **2005**, 25, 229.10.

11. Giampa`, C.; Middei, S.; Patassini, S.; Borreca, A.; Marullo, F.; Laurenti, D.. *Eur. J. Neurosci.* **2009**, 29, 902.

12. Fujimaki, K.; Morinobu, S.; Duman, R.S. *Neuropsychopharm*, **2000**, 22, 42.

13. Li, Y.F.; Huang, Y.; Amsdell, S.L.; Xiao, L.; O'Donnell, J.M.; Zhang, H.T. *Neuropsychopharm*, **2009**, 34, 2404.

14. Nikulina, E.; Tidwell, J.L.; Dai, H.N.; Bregman, B.S.; Filbin, M.T. *Proc Natl Acad Sci,* **2004**, 101, 8786.

15. O'Donnell, J.M.; Zhang, H.T. *Trends Pharmacol. Sci.* **2004**, 25, 158.

16. Torphy, T. *Am. J. Resp. Crit. Care Med.* **1998**, 157, 351.

17. Spina, D. *Br J Pharmacol.* **2008**, 155, 308.

18. Rabe, K. F. *Br. J. Pharmacol.* **2011**, 163, 53.

19. Keravis, T.; Monneaux, F.; Yougbaré, I.; Gazi, L.; Bourguignon, J.J.; Muller, S.; Lugnier C. *PLoS ONE.* **2012**, 7.

20. Wittmann, M.; Helliwell, P.S. *Dermatol. Ther.* **2013***,* 3,1.

21. Park, S.J.; Ahmad, F.; Philp, A.; Baar, K.; Williams, T.; Luo, H.B.; Ke, H.M.; Rehmann, H.; Taussig, R.; Brown, A.L.; Kim, M.K.; Beaven, M.A.; Burgin, A.B.; Manganiello, V.; Chung, J.H. *Cell*, **2012**, 421.

22. Zhu, J.; Mix, E.; Winblad, B. *CNS Drug Rev,* **2001**,7, 387.

23. DailyMed. Forest Laboratories, Inc. August 2013. Retrieved 13 November 2013.

24. Lugnier, C. *Curr. Opin. Pharmacol*. **2011**, 11, 698.

25. Hotamisligil, G. S. *Nature*. **2006**, 444, 860.

26. Frey, U.; Huang, Y.Y.; Kandel, E.R. *Science*. **1993**, 260,1661.

27. Matthies, H.; , K.G. *Neuroreport.* **1993**, 4,712.

28. Kodimuthali, A.; Jabaris, S.S.L.; Pal, M. *J. Med. Chem.* **2008**, 18,5471.

29. Beghè, B.; Rabe, F.; Fabbri, L. M. *Am. J. Respir. Crit. Care Med.* **2013**, 188, 271.

30. Man, H.; Schafer, P.; Wong, L.M.; Patterson, R.T.; Corral, L.G.; Raymon, H.; Blease, K.; Leisten, J.; Shirley, M.A.; Tang, Y.; Babusis, D.M.; Chen, R.; Stirling, D.; Muller, G.W. *J. Med. Chem.* **2009***,* 52,1522.

31. Brooks, M. *Medscape Medical News (WebMD)*. Retrieved 28 March **2014**

32. Pagès, L.; Gavaldà, A.; Lehner, M. D. *Expert Opin. Ther. Pat*. **2009**, 19, 1501.

33. Gavaldà, A.; Roberts, R. S. *Expert Opin. Ther. Pat*. **2013**, 23, 997.

34. Schudt, C.; Winder, S.; Eltze, M.; Kilian, U.; Beume, R. *Agents Actions Suppl.* **1991**, 34, 379.

35. Card, G.L.; England, B.P.; Suzuki, Y.; Fong, D.; Powell, B.; Lee, B.; Luu, C.;

Tabrizizad, M.; Gillette, S.; Ibrahim, P.N.; Artis, D.R.; Bollag, G.; Milburn, M.V.; Kim, S.H.; Sclessinger, J.; Zhang, K.Y. *Structure,* **2004**, 12, 2233.

36. Van der Mey, M.; Hatzelmann, A.; Van der Laan, I.J.; Sterk, G.J.; Thibaut, U.; Timmerman, H. Novel selective PDE4 inhibitors. 1. *J Med Chem*. **2001**, 44, 2511.

37. Schmidt, B.; Scheufler, C.; Volz, J.; Feth, M.P.; Hummel, R.; Hatzelmann, A.; Zitt, C.; Wohlsen, A.; Marx, D.; Kley, H.; Ockert, D.; Heuser, A.; Christiaans, J.A.M.; Sterk, G.J.; Menge ,W.M.P.B. Patent WO2008/138939 A1, **2008**.

38. As assessed by substructure searches of E-molecules (http://www.emolecules.com), Reaxys [Reller, T. **2009**] and SciFinder [Chemical Abstracts Service: Columbus, **2015**].

39. Stegemann, S. *Eur. J. Pharm. Sci.* **2007**, 31, 249.

40. Hann, M.M.; Keserü, G.M. *Nature rev*, **2012**, 11, 355.

41. Hoffmann, E.; Wermuth, C.G.; Cahn, J. Patent DE2162092, **1972**.

42. Beesley, R.M.;Ingold, C.K.; Thorpe, J.F. *J. Chem. Soc.* **1915**, 107, 1080.

43. Bourguignon, J.J.; Lagouge, Y.; Lugnier, C.; Klotz, E.; Macher, J.P.; Raboisson, P.; Schultz, D.; Patent US2004/152888. **2004**.

44. Cooper, N.; Teixeira, M. M.; Warneck, J.; Miotla, J. M.; Wills, R.E.; Macari, D. M.; Gristwood, R. W.; Hellewell, P. G. *Br. J. Pharmacol.* **1999**, 126, 1863.

Graphical abstract

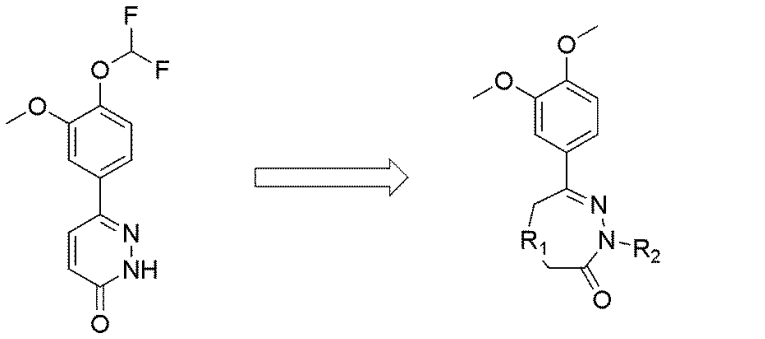

Zardaverine
PDE4 IC_{50} = 1.41 μM

R_1 = CH_2, *gem*-CH_3; 28 examples
PDE4 IC_{50} = 0.17 - 13 μM